

H. S. Köhler<sup>1</sup>*Physics Department, University of Arizona, Tucson, Arizona 85721, USA***Abstract**

Efimov physics relates to 3-body systems with large 2-body scattering lengths  $a_s$  and small effective ranges  $r_s$ . For many systems in nature the assumption of a small effective range is not valid. The present report shows binding energies  $E_3$  of three identical bosons calculated with 2-body potentials that are fitted to scattering data and momentum cut-offs  $\Lambda$  by inverse scattering. Results agree with previous works in the case of  $r_s \ll a_s$ .

While energies diverge with  $\Lambda$  for  $r_s = 0$ , they converge for  $r_s > 0$  when  $\Lambda > \sim 10/r_s$ . With  $a_s^{-1} = 0$  the converged energies are given by  $E_3^{(n)} = C_0^{(n)} r_s^{-2}$  with  $n$  labelling the energy-branch and calculated values  $C_0^{(0)} = 0.77, C_0^{(1)} = .0028$ . This gives a ratio  $\sim 278$  thus differing from the value  $\sim 515$  in the Efimov case.

Efimov's angular dependent function is calculated. Good agreement with previous works is obtained for  $r_s \ll a_s$ . With the increased values of  $r_s$  the shallow states still appear Efimov-like. For deeper states the angular dependence differs but is independent of  $r_s$ .

## 1 Introduction

Systems involving particles with 2-body interactions at or close to the Unitary limit have become of specific interest in the physics community during the last several years for reasons that have repeatedly been pointed out in numerous publications related to both atomic and sub-atomic problems. The Unitary limit is here defined as being that for which the scattering length  $a_s$  and the effective range  $r_s$  is infinite and zero respectively.

In this regard the bound system of three bosons is of special interest. This was first brought to the attention by the works of Thomas [2] and of Vitali Efimov [3, 4]. Bosons interacting with a resonance in the 2-body state (i.e.  $a_s^{-1} \sim 0$ ) result in a strongly bound three-body system *and* with a spectrum of loosely bound excited states.

The literature has brought to the attention several systems in nature for which these findings are relevant.

On the theoretical side the application of Effective Field Theory (EFT) methods have been proven very powerful [5, 6, 7, 8, 9, 10] for a theoretical interpretation. The main focus has been on short-ranged potentials at or near the Unitary limit for which  $r_s \ll a_s$ , but more recent EFT publications include effective range corrections [11, 12].

A rather different approach is used here. The inverse scattering formalism for separable potentials is used to construct potentials as functions of the scattering parameters as well as 2-body binding energy, and renormalised by a cut-off in momentum-space. The potential in the Unitary limit, a renormalised  $\delta$ -function (in coordinate) space, is of specific interest. The results presented below agree with previous Efimov physics calculations for  $r_s = 0$ . The  $r_s > 0$  results do in general show some qualitative differences.

The present investigation focuses on Efimov energies and the Efimov function, dependence on scattering length and in particular on the effective range. Some preliminary results were given in ref. [13].

Scaling properties are a main thread in this work.

In Section 2 is found a presentation of the necessary tools which are the Faddeev equation and the inverse scattering method. Section 3 show results of numerical calculations in 4 subsections with 8 Figures. Section 4 is a summary and some discussion of the results. Some relations regarding off-shell scattering and three-body forces are shown in Appendix A, while Appendix B shows an important relation pertaining to scattering and the separable interaction in the Unitary limit.

## 2 Formalism

### 2.1 Two-body Separable Interaction

The input for the calculations in this report are scattering phase-shifts  $\delta(k)$  related to the scattering length  $a_s$  and an effective range  $r_s$  by

$$k \cot \delta(k) = -\frac{1}{a_s} + \frac{1}{2} r_s k^2 \quad (1)$$

---

<sup>1</sup>e-mail: kohlers@u.arizona.edu

A momentum cut-off  $\Lambda$  will also be defined so that

$$\delta(k > \Lambda) = 0$$

With the scattering parameters chosen so that the phase-shifts do not change sign, as will be the case here, they can be reproduced by a rank-1 separable potential

$$V(k, k') = -v(k)v(k') \quad (2)$$

that is obtained by inverse scattering from[14]

$$v^2(k) = \frac{4\pi}{k} \sin \delta(k) |D(k^2)| \quad (3)$$

where

$$D(k^2) = \frac{k^2 + E_B}{k^2} \exp \left[ \frac{2}{\pi} \mathcal{P} \int_0^\Lambda \frac{k' \delta(k')}{k^2 - k'^2} dk' \right] \quad (4)$$

where  $\mathcal{P}$  denotes the principal value. The interaction is fully defined by the phase-shifts and the two-body binding energy  $E_B$ . Note that the two fits, to scattering and to binding energy are independent. The equation

$$\sqrt{E_B} = (1 - \sqrt{1 - 2r_s a_s^{-1}}) \frac{1}{r_s} \quad (5)$$

relates  $E_B$  to  $[a_s, r_s]$  but only for  $r_s \ll a_s$  and it is not useful for the calculations below. In the limit  $r_s = 0$  it reduces to

$$E_B = a_s^{-2}$$

which will be used also when  $r_s \neq 0$  together with  $E_B = 0$  for  $a_s < 0$ . This simplifies the comparison with the  $r_s = 0$  calculations in these preliminary calculations. The major importance is that the 2-body system *has* a bound state.<sup>2</sup>

When dealing with some specific physical system one (in general) knows or assumes some binding-energy, but this is not the case here. The expression (5) for the binding energy does not introduce another parameter in the theory, being a function of  $a_s$  and  $r_s$  only, but if in some specific case one would tune the binding energy say by some shape-parameter there would be another parameter to consider.

### 2.1.1 Unitary Limit

A well-known reason for *assuming* a separable interaction in 3- and other many-body works is that it in general simplifies the formalism as well as the numerical calculations. There is however a particular case where the interaction IS separable. Namely that when the 2-body system has a bound state at or close to zero[16], which is the case in the Unitary limit.

The principal value integration in eq. (4) can be done analytically for  $\delta(k)=\text{constant}$ . The Unitary limit is a special case with  $\delta(k) = \frac{\pi}{2}$ , for which the rank-1 separable potential  $v_u(k)$  is given by [15]

$$v_u^2(k) = -\frac{4\pi}{(\Lambda^2 - k^2)^{\frac{1}{2}}} \quad (6)$$

If  $\Lambda \gg k$  one finds

$$v_u^2(k) \rightarrow -\frac{4\pi}{\Lambda} \quad (7)$$

In this limit, *but only in this limit*, the unitary interaction is independent of momentum and a  $\delta$ -function in coordinate space with the strength inversely proportional to the cut-off. But for the finite values of  $\Lambda$  needed for computations, renormalisation is required resulting in  $v_u$  as given by eq. (6). Note that there is then an abrupt increase in strength and a singularity as  $k \rightarrow \Lambda$ . This is required to preserve the condition  $\delta = \frac{\pi}{2}$  for all  $k \leq \Lambda$ , as required for the Unitary limit. (See Appendix B.)

The singularity can cause numerical problems that however can be largely overcome by proper computational methods. The substitution

$$k = \Lambda \sin \theta,$$

---

<sup>2</sup>Calculations showed no qualitative difference if using eq. (5).

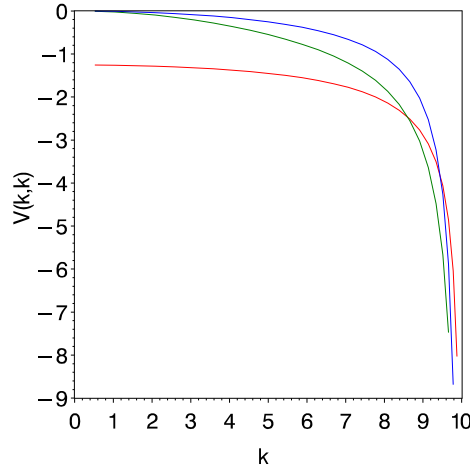


Figure 1: Lowest curve (red on-line) shows the diagonal of the Unitary interaction in momentum-space. The two other curves are, from below, the potentials for  $a_s = 10$  (green on-line) and for  $a_s = 20$  (blue on-line). All three are with the effective range  $r_s = 0$ .

with  $\theta$  the new variable, can for example be helpful yielding

$$v_u^2(\theta) = -\frac{4\pi}{\Lambda \cos \theta} \quad (8)$$

which is used successfully in the computations.<sup>3</sup> Fig. 1 shows the Unitary interaction (lowest curve) and for comparison two other potentials with  $a_s = 10$  and 20 respectively.

## 2.2 The Many-body System

A rank-1 potential is often sufficient to fit the on-shell data at low energy as is done in this report. The off-shell and off-diagonal parts of the T-matrix is then fixed by default.

On-shell relates to the asymptotic form of the two-body scattering wave-function, while off-shell relates to the interior wave-function, i.e. to correlations in the two-body system. One may however like to change the off-shell behaviour. This can be done by extending to a rank-2 (or higher) potential (which implies introducing another parameter), while preserving the on-shell fit. This provides a practical tool for exploring off-shell effects on many-body properties.<sup>4</sup>

The 3-boson system collapses in the Unitary limit (the energy diverges) with  $\Lambda$ . This is well-known. In ref.[5] this collapse was remedied by adding a 3-body force. It was shown in ref.[13] that the same could be accomplished by a change in off-shell scattering with a rank-2 potential as described above.

In each of these methods the high energy (ultraviolet) region of the interaction was modified; in one case by a three-body force in the other by a change in off-shell scattering.

Although the two methods have a similar 'end-result' it is important to understand that in each case there is a different physics involved. (Appendix A.)

Findings below show that the effective range also has the effect of preventing a collapse. This is not completely un-expected as it explicitly introduces a finite range parameter into the system.

<sup>3</sup>This is in particular useful because  $dk \rightarrow \Lambda \cos \theta d\theta$  which can eliminate the  $\cos \theta$  in the denominator of (8)

<sup>4</sup>It was for example used by the author in earlier work on the triton. [17]

## 2.3 Faddeev Equation

The Faddeev three-boson equation for a spin-independent rank-1 separable potential is given by

$$\chi(q) = \frac{2}{\mathcal{I}(E_3 - \frac{3}{4}q^2)} \int_0^{2\Lambda} \frac{v(|\mathbf{k} + \frac{1}{2}\mathbf{q}|)v(|\mathbf{q} + \frac{1}{2}\mathbf{k}|)}{q^2 + \mathbf{q} \cdot \mathbf{k} + k^2 - E_3} \chi(k) d\mathbf{k} \quad (9)$$

with

$$\mathcal{I}(s) = 1 + \frac{1}{2\pi^2} \int_0^\Lambda v^2(k)(s - k^2)^{-1} k^2 dk \quad (10)$$

With the phase-shifts defined, as announced above, in terms of two scattering parameters and the cut-off  $\Lambda$  one will have  $E_3 = E_3(a_s, r_s, \Lambda)$ . In the present investigation the scattering parameters  $[a_s, r_s]$  are considered *internal* parameters defining the 3-body system, while  $[\Lambda]$  is considered an *external* parameter if possible chosen larger than the maximum momenta of the bound particles. This means in general that one has to choose  $\Lambda > 1/R$  with  $R$  being the physical size of the system. This size is a 'functional' of the interaction (the internal parameters) and so is therefore  $\Lambda$ . As an example, the three-body system collapses in the Unitary limit, with  $\Lambda \rightarrow \infty$ , a well-known divergence.

Three separate cases will be considered here with results presented in three separate sections. The first will be the Unitary limit i.e. both  $r_s$  and  $a_s^{-1} = 0$ . The second is  $a_s^{-1} \neq 0$  while  $r_s = 0$  and the third the more general case, both  $r_s$  and  $a_s^{-1} \neq 0$ . The purpose of the present investigation is in particular to investigate the latter case, with  $r_s > 0$ .

## 3 Numerical Results

### 3.1 Unitary Limit

The Unitary limit is a special case. After a change of variables (see above),  $k \rightarrow \Lambda \sin \theta$ , the function  $\mathcal{I}(s)$ , eq. (10), becomes

$$\mathcal{I}(s) = 1 + \frac{2}{\pi} \mathcal{P} \int_0^{\frac{\pi}{2}} \sin^2 \theta (s - \sin^2 \theta)^{-1} d\theta \quad (11)$$

The integral, done analytically for  $s < 0$  yields

$$\mathcal{I}(s) = -\frac{s}{\sqrt{s^2 - s}} \quad (12)$$

(See Appendix B for  $s > 0$ ). The only free parameter in the Unitary limit is  $\Lambda$  so that one has  $E_3 = E_3(\Lambda)$ . It is then convenient in this case to choose momenta and energies in units of  $\Lambda$  and  $\Lambda^2$  respectively by substitutions  $k \rightarrow k\Lambda$   $q \rightarrow q\Lambda$  and  $E_3 = E_u\Lambda^2$  in eq. (9) to get with eq. (12) and  $s = E_u - \frac{3}{4}q^2$

$$\chi(q) = -\frac{2\sqrt{s^2 - s}}{s} \int_0^2 \frac{v_u(|\mathbf{k} + \frac{1}{2}\mathbf{q}|)v_u(|\mathbf{q} + \frac{1}{2}\mathbf{k}|)}{q^2 + \mathbf{q} \cdot \mathbf{k} + k^2 - E_u} \chi(k) d\mathbf{k} \quad (13)$$

With  $n$  labelling a specific state with energy  $E_u^{(n)}$  the eigenvalue spectrum in this Unitary limit was calculated with the result (in units of  $\Lambda^2$ ):

$$E_u^{(0)} = -.1325, \quad E_u^{(1)} = -.0002520, \quad E_u^{(2)} = -.0000004568$$

One finds

$$E_u^{(0)}/E_u^{(1)} = 515$$

agreeing with the Efimov result while

$$E_u^{(1)}/E_u^{(2)} = 630$$

This latter discrepancy is ascribed to computational inaccuracies that increases for the smaller energy. ( $E_u^{(2)} = -.0000004893$  would be the 'correct' value.)

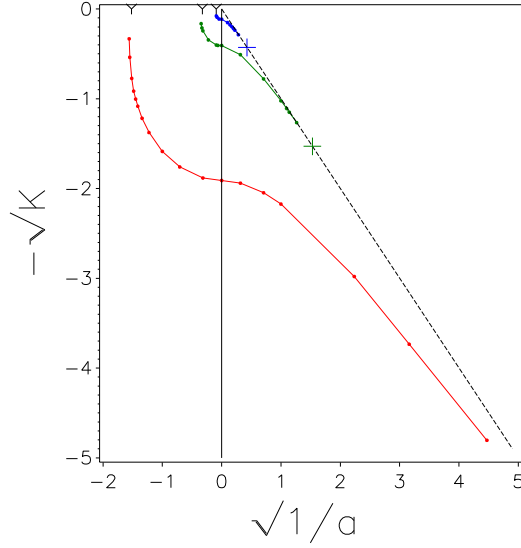


Figure 2: Energy as a function of scattering length  $a_s$  while the effective range is  $r_s = 0$ . Following convention,  $K \equiv \kappa = \sqrt{E_3}$ . The lowest curve (red on-line) is for  $n = 0$ . The two other curves (green and blue respectively on-line) are for  $n = 1$  and  $2$  respectively. The crosses on the dimer-energy line, shown by the broken line, are explained in the text.  $\Lambda = 10$  in this plot.

### 3.2 Non-zero Scattering Length but Zero Effective Range

In this second scenario with  $r_s = 0$  while  $a_s \neq 0$  one will have  $E_3 = E_3(a_s, \Lambda)$ . This case has been the focus of numerous investigations since the early works of Thomas and Efimov; in particular as relates to experimental studies of cold atoms and the ability to tune the scattering length with the aid of Feshbach resonances.

Results of Faddeev calculations are shown in Fig. 2. Following convention, the figure shows  $E_3^{\frac{1}{4}}$  vs  $a_s^{-\frac{1}{2}}$  (with appropriate signs) for three separate branches cutting the  $a_s = 0$  axis at the values shown above. With  $\kappa_* = \sqrt{E_3(a_s^{-1} = 0)}$  for each branch it has been found, e.g. [7], that the energies should approach zero for  $a'_s \sim -1.56\kappa_*^{-1}$ . These scattering lengths are indicated by a "Y" for each of the states and largely agree with the calculations. Furthermore, the trimer and dimer energies are estimated to coincide at  $a_* = 0.0707645086901\kappa_*^{-1}$ . These points are shown by crosses in Fig. 2 for the two shallow states. For the lowest state the corresponding point is predicted to be at  $a_s^{-1} \approx 51$ .

It is convenient to choose  $\Lambda$  as the unit of momentum and introducing the dimensionless variable  $a_s\Lambda$ . The phase-shifts and therefore the potential are then functions of this variable. So in addition to the  $\Lambda^2$  factor the energy will also be a function of the same variable. One will have

$$E_3^{(n)} = \Lambda^2 F^{(n)}(1/\Lambda a_s) \quad (14)$$

where as before  $n$  labels a specific (Efimov) branch. (The reason for choosing the inverse of  $\Lambda a_s$  becomes obvious below.) While Fig. 2 shows the energy vs  $a_s$  for  $\Lambda = 10$  the energy for any other value of  $\Lambda$  and  $a_s$  can be obtained from eq. (14). Of interest is then the function  $F^{(n)}$ . The full line in Fig. 3 shows  $\sqrt{F^{(n)}(1/\Lambda a_s)}$  for  $n = 0$ , the deeper state in Fig. 2. It is seen that this function is to some approximation a linear function with the slope (derivative) being approximately one. The function  $F^{(1)}$  is a (nearly) scaled copy of  $F^{(0)}$  the scaling factor being 22.7, as shown by the dotted line in Fig. 3. The reason for displaying these functions is for comparison with the similar situation when  $r_s \neq 0$  that is shown in Sect. 3.4.

From the functions  $F^{(n)}$  one can calculate the energies  $E_3$  for any other variables  $a_s$  and  $\Lambda$  for each branch  $n$ . These functions can of course also be calculated directly from the Efimov Universal function,  $\Delta(\xi)$ . It is related to the energy  $E_3$  by

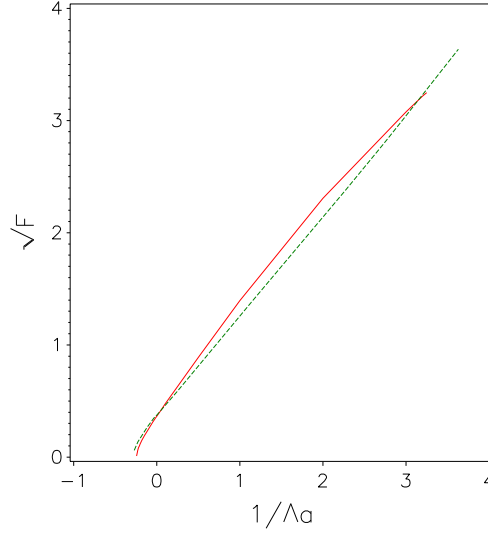


Figure 3: The function  $\sqrt{F^{(n)}}$  is shown for the two deepest states. The full curve (red on-line) is for  $n = 0$  while the broken (green on-line) is for  $n = 1$ . This curve has been scaled up by the Efimov factor 22.7 as a result of which the two curves are close. Note also the approximately linear function of  $1/a_s\Lambda$ .

$$E_3^{(n)} = -a_s^{-2} + \kappa_*^2 (e^{-\frac{2\pi}{s_0}})^{n-n_0} e^{\frac{\Delta(\xi)}{s_0}} \quad (15)$$

where  $s_0 \approx 1.00624$  and  $n$  labels a specific Efimov branch and  $n_0$  that branch for which  $\kappa_*^2 = E_3(a_s^{-1} = 0)$ . The angle  $\xi$  is defined by

$$\tan \xi = -a_s \sqrt{E_3^{(n)}} \quad (16)$$

It is easily seen that because of the scaling relation shown above  $\Delta(\xi)$  is indeed a function of  $\xi$  only, independent of  $\Lambda$ .

$\Delta(\xi)$  was calculated with twelve significant figures by Mohr[9]. Earlier results by Braaten et al [6] were shown parametrized in their publication.

The dots and crosses in Fig. 4 show  $\Delta(\xi)$  calculated from eq.(15) using the same energies as used for Fig. 2. The crosses refer to the energy  $E^{(0)}$ , the deepest state, and the dots to  $E^{(1)}$ , the next shallower state. The broken line is from the parametrisation given in ref [6]. The present calculations are not of high-precision but the difference between our result and those of ref. [6] are still less than a few percent.

### 3.3 Non-Zero Effective Range and Zero Scattering Length

After having verified that the  $r_s = 0$  calculations with the separable interactions agree with previous works the results with  $r_s \neq 0$  can now be presented.

The scenario changes drastically with the introduction of a non-zero effective range. As a preliminary to the more general case the scattering length is first assumed to be infinite. The remaining variables are then  $r_s$  and  $\Lambda$ . While in the previously considered case  $E_3 \propto \Lambda^2$  associated with a collapse of the system (in coordinate space), the range-parameter  $r_s$  now provides some finite size  $R$  of the system under consideration. As is to be expected computations of  $E_3$  as a function of  $\Lambda$  now show a convergence for  $\Lambda > 1/R$ . With  $\Lambda$  providing a momentum scale and following arguments above one can expect a relation of the following form

$$E_3^{(n)} = \Lambda^2 F_0^{(n)}(r_s \Lambda) \quad (17)$$

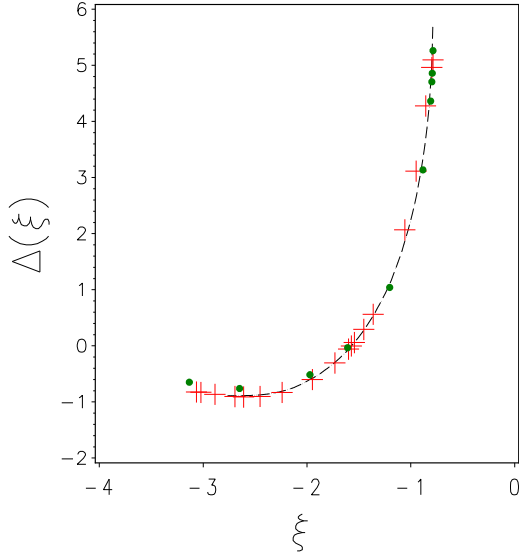


Figure 4: The function  $\Delta(\xi)$  is shown. The crosses (red online) are for  $n = 0$  the dots (green on-line) are for  $n = 1$ . The broken line (black on-line) shows the results of ref.[6].

In order for convergence one must then have

$$F_0^{(n)}(r_s \Lambda) \rightarrow \frac{1}{(r_s \Lambda)^2} \quad (18)$$

for large  $\Lambda$ . The energy of the three body system will then scale with  $r_s$  as

$$E_3^{(n)} = \frac{C^{(n)}}{r_s^2}$$

for  $\Lambda$  large. The coefficients  $C^{(n)}$  were calculated to get  $C^{(0)} = 0.770$  and  $C^{(1)} = 0.00298$ . The ratio  $C^{(0)}/C^{(1)} \simeq 278$  differs from the related ratio of 515 for Efimov states.

Fig. 5 shows  $E_3^{(0)}$  and  $278 * E_3^{(1)}$  as a function of  $\Lambda$  for  $r_s = 0.1$ . The energy for any other values of the parameters  $r_s \neq 0$  and  $\Lambda$  can be calculated by the help of eq. (17). Calculations have shown that the energy converges to the asymptotic value at a critical value

$$\Lambda_c \sim 10/r_s$$

as in Fig.5 where one finds  $\Lambda_c \sim 100$  for  $r_s = 0.1$ .<sup>5</sup>

### 3.4 General Case

The main inspiration for the present work has been to find the effect of a non-zero effective range  $r_s > 0$  together with an inverse scattering length  $a_s^{-1} \neq 0$  as opposed to the case when  $r_s = 0$ .

There is an additional factor to address here, the dimer (two-body) binding energy. In the inverse scattering theory with separable interactions it is chosen separate, independent of the fit to scattering data. Following the discussions in Sect. 2.1 the choice here is  $E_B = a_s^{-2}$ . Any other choice might change our results but (probably) only in a quantitative way. In cases of real physical systems one would of course choose the appropriate dimer binding energy assumed known for the particular system under consideration. One consequence of this choice

<sup>5</sup>Fig. 3 in ref.[13] shows  $E$  vs  $\Lambda$  for  $r_s = .0, .03, .05$  and  $.1$  with convergence at  $\Lambda_c \sim 10/r_s$ . The convergence  $\Lambda_c$ , as a function of  $r_s$  is also seen. The curves for  $a_s^{-1} = 0$  (excluding the  $r_s = 0$ ) are related by the scaling in eq. (17)

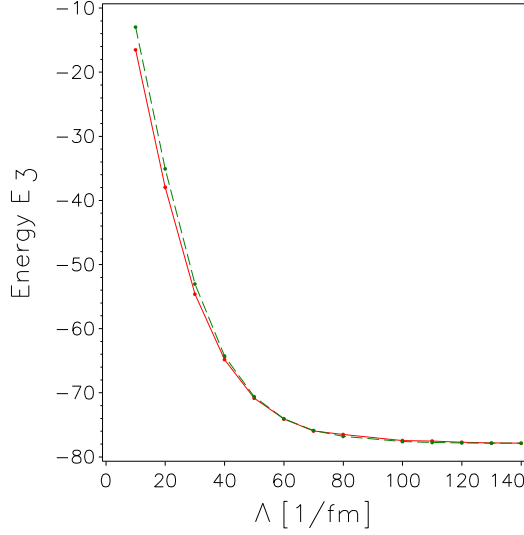


Figure 5: The energies  $E_3^{(0)}$  (red on-line) and  $E_3^{(1)}$  (green on-line) are shown here as a function of the momentum cut-off  $\Lambda$  with the effective range being  $r_s = 0.1$  while  $a_s^{-1} = 0$ . The energy  $E_3^{(1)}$  is multiplied with the factor "278" (see text) and the two energies practically overlap. The energy for any other  $[\Lambda, r_s]$  is obtained by the scaling shown in the text. Of particular interest is the asymptotic value, i.e.  $\Lambda > \Lambda_c$ , that scales as  $r_s^{-2}$ .

is that no additional parameter is introduced in the calculations. With  $\Lambda > \Lambda_c$  (see above) the energy is then a function only of  $a_s$  and  $r_s$ . Choosing momenta in units of  $r_s^{-1}$  the potential will be a function of the dimensionless parameter  $a_s/r_s$ . The energy  $E_3$  then has to have the form:

$$E_3^{(n)} = r_s^{-2} F_1^{(n)}(r_s a_s^{-1}) \quad (19)$$

where the functions  $F_1^{(n)}$  are to be determined computationally.<sup>6</sup> The scaling shown here is analogous to that shown in eq. (14), with  $r_s$  replacing  $\Lambda$  and providing the new momentum scale.

Fig. 3 showed functions  $F^{(n)}(1/\Lambda a_s)$ . The similar functions  $F_1^{(n)}(r_s/a_s)$  are shown in Fig. 6. The function  $F_1^{(1)}$  maps onto  $F^{(1)}$  in Fig. 3, with a scaling factor of  $\sim 3$ . So Efimov physics seems to apply for the shallow state. With regard to the deeper state there are some qualitative similarities but there are definitely quantitative differences. Rather than having a slope  $\sim 1$  as in the Efimov case, Fig. 6 shows  $\sqrt{F_1^{(0)}}$  to have a slope of  $\sim 1.5$ .

All the results in this section, for  $r_s \neq 0$  can be obtained by scaling from the functions  $F_1^{(n)}$  shown in Fig. 6. As a first example is shown Fig. 7, the energy vs  $a_s$  for  $r_s = 0.1$ . These curves are seen to be qualitatively similar to the 'Efimov-curves' shown by Fig. 2. From these data a function  $\Delta'(\xi)$  was calculated using eq. (15) with the result shown in Fig. 8. There is a factor  $(e^{-\frac{2\pi}{s_0}})^{n-n_0} = 515^{n-n_0}$  in eq. (15) for  $\Delta(\xi)$ . For the purpose of calculating  $\Delta'(\xi)$  it was replaced by  $278^{n-n_0}$ . The function  $F_1^{(0)}$  generated the result shown by the crosses, while  $F_1^{(1)}$  the dots. The dots, referring to the shallowest state spans  $r_s/a_s < 0.8$ . They coincide with the Efimov  $\Delta(\xi)$  (the broken line), while there is a definite difference for the deeper state derived from  $F_1^{(0)}$ .

The situation here is however analogous to that in sect. 3.2. There, the consequence of the scaling expressed by eq. (14) had as a result that the calculation of  $\Delta(\xi)$  was independent of  $\Lambda$ . The scaling expressed by eq. (19) can formally be obtained by replacing  $\Lambda$  in eq. (14) by  $r_s$ . The function  $\Delta'(\xi)$  is similarly independent of  $r_s$ .

<sup>6</sup>Like in Sect. 3.2 for the function  $F$  the argument of  $F_1$  is chosen as the inverse of  $a_s/r_s$ .



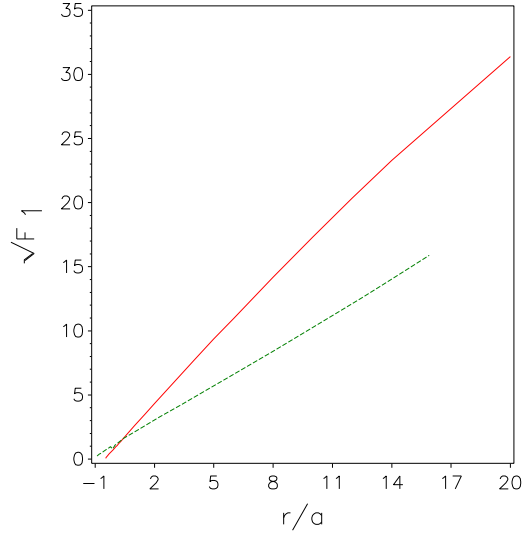


Figure 6: The full curve (red on-line) shows  $\sqrt{F_1^{(0)}}$  as a function of  $r_s a_s^{-1}$ . The broken curve (green on-line) shows  $\sqrt{F_1^{(1)}}$  scaled up as in Fig. 3. It is seen that it (the broken) only spans values of  $r/a < 1$  (note the scaling factor "22.7") so that Efimov physics would or might apply here. The full line, for  $n = 0$ , (red on-line) includes energies for  $r_s/a_s = 20$  and there is as a consequence an apparent deviation from Efimov physics here. This is substantiated by the results shown in Fig. 8.

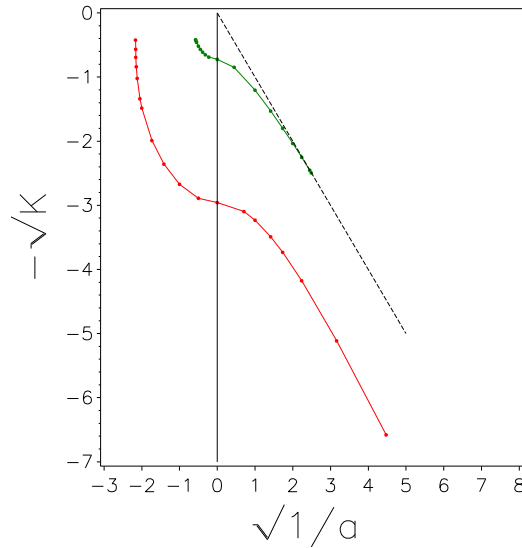


Figure 7: Energy ( $K$ ) as a function of scattering length for  $r_s = 0.1$ . The energy ratio between the two states at  $1/a = 0$  is here  $\sim 278$ . This factor is independent of  $r_s$ . It is approximate and improved calculations are called for.

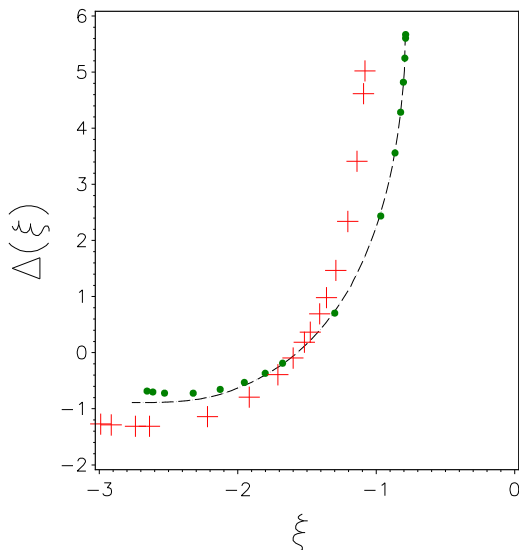


Figure 8: The function  $\Delta'(\xi)$  calculated from eq. (15), with "515" replaced by "278" as described in text, for each of the two states shown in Fig. 7. This function is independent of the value of the effective range  $r_s$ . The dots (green on-line) refers to the shallow state, while the crosses (red on-line) the deeper. The broken line (black on-line) shows the Efimov function using the parametrization in ref.[6].

## 4 Summary

Bound state energies  $E_3$  of the 3-boson system with 2-body interactions at or close to the Unitary limit were calculated with the Faddeev equation in momentum-space. Separable potentials were obtained by inverse scattering as a function of scattering length  $a_s$ , effective range  $r_s$  and momentum cut-off  $\Lambda$ .

In the Unitary limit ( $r_s = a_s^{-1} = 0$ ) three branches (labelled  $n = 1 - 3$ ) were identified with energies  $E_3^{(n)}$  (in units of  $\Lambda^2$ ),  $-.1325$ ,  $-.000252$ ,  $-.00000045668$  respectively. The ratio  $E_3^{(n-1)}/E_3^{(n)} \sim 515$  in agreement with theory.

With  $r_s = 0, a_s \neq 0$  (Sect. 3.2) the energy for each branch scales as  $E_3^{(n)} = \Lambda^2 E^{(n)}(a_s \Lambda)$ . Efimov's function  $\Delta(\xi)$  was calculated separately for two branches ( $n = 1, 2$ ) with the result shown in Fig. 4 agreeing with previous works [6, 9].

While the energy  $\propto \Lambda^2$  for  $r_s = 0$  the situation changes when  $r_s > 0$ . One still finds the energy  $\propto \Lambda^2$  for small  $\Lambda$  but it converges for  $\Lambda > \Lambda_c \sim 10/r_s$  as seen in Fig. 5 (Sect.3.3) for  $a_s^{-1} = 0$ . It was shown that the energy converges to  $E_3(n) = C^{(n)} r_s^{-2}$  with  $r_s^{(-1)}$  being the only remaining momentum-scale with  $\Lambda > \Lambda_c$ . The ratio  $C^{(n-1)}/C^{(n)}$  is calculated to be  $\sim 278$  differing from the corresponding Efimov value  $\sim 515$ .

It was shown in Sect. 3.4 that if both  $r_s > 0$  and  $a_s^{-1} \neq 0$  the energy can be written as  $E_3^{(n)} = r_s^{-2} F_1^{(n)}(r_s a_s^{-1})$ . The function  $F_1^{(n)}$  was shown and a function  $\Delta'(\xi)$  was calculated analogous to the Efimov function  $\Delta(\xi)$ . Fig. 8 shows it to overlap with the Efimov for the shallow state. This might be explained by the fact that for this state,  $r_s$  is still  $< a_s^{-1}$ . For the deeper state, there is however a definite difference even for that range of  $a_s$ . An important result following from the expression (19) for the energy  $E_3^{(n)}(r_s, a_s)$  is however that  $\Delta'(\xi)$  is independent of  $r_s > 0$  also for these states. Further investigation is asked for here.

There would (probably) be some quantitative changes in the results above if a different algorithm were used for the binding energy as a function of  $a_s$  and  $r_s$ , but this all relates to a specific system, beyond the scope of the present investigation. It would in general introduce another parameter into the theory.

The Efimov physics, valid for  $r_s/a_s \ll 1$  is well understood and explained by various methods. Particularly powerful is the EFT approach with recent and on-going research[11, 12] extending this method to finite values of the effective range.

The main purpose of this work is to provide an alternative approach to the the problem at hand and in particular to explore the domain of  $r_s > 0$ . The results were obtained with rank-1 separable potentials. It is to be expected that any other potential fitted to the same scattering data would give the same, or very similar, results.

Although much care was taken, the computing was not of 'high precision' and could be improved upon, but this is not expected to have an impact on qualitative conclusions.

## 5 Appendix A

The  $\mathcal{R}$  (or  $\mathcal{T}$ )-matrix relates the potential to observable scattering data while the potential in itself is not an observable. The phase-shifts  $\delta(k)$  are related to the reactance matrix  $\mathcal{R}$  and indirectly to the two-body interaction  $V$  by

$$\begin{aligned}\mathcal{R}(\omega) &= V + VP \frac{1}{\omega - k'^2} \mathcal{R}K \\ < k | \mathcal{R}(\omega = k^2) | k > = \frac{1}{k} \tan \delta(k)\end{aligned}\tag{20}$$

As a consequence only *diagonal* elements of the  $\mathcal{R}$ -matrix can be obtained from the phase-shifts and only for  $\omega = k^2$ . In addition, experimental information puts an upper limit on  $k$ . A large part of the matrix is therefore beyond direct experimental reach. Many-body theories do in general need more, requiring some other input, e.g. by potential models.

An important example is off-shell information. Off-shell implies  $\omega \neq k^2$ . It is therefore relevant to consider

$$\begin{aligned}\frac{\partial \mathcal{R}}{\partial \omega} &= \langle \Psi - \Phi | \Psi - \Phi \rangle = I_w \\ \Psi &= \Phi + \frac{1}{\omega - k'^2} V \Psi\end{aligned}\tag{21}$$

where  $\Phi$  is the unperturbed wave-function.

These relations were already used by Moszkowski and Scott.[18, 19]  $I_w$  is often referred to in the literature as the wound-integral. The 'correlated' wave-function  $\Psi$  relates to details of the interaction (even beyond what may be available from experiments.)

Assume a many body system with 2-body interactions only; no 3-body (or  $n$ -body,  $n > 2$ ) forces. Then consider two particles (i,j) interacting in this system. The interaction would be off-shell,  $\omega \neq k^2$ , mainly because of binding-effects, meaning that other particles (k) affect the the interaction between (i,j). So to calculate something, e.g the total energy, one would have to sum over (i,j,k) that 'looks' as if one is dealing with a 3-body *force*, although 2-body only was assumed. It is then more appropriate to say one is dealing with 3-body *terms* not *forces*. Whether the 3-body term is 'important' or not is another question. There are of course in principle also 4,5 etc body terms. That depends on the system in question including density, temperature etc.

The above is to illustrate the popular statement of equivalence between the off-shell effect and that of a 3-body force, even though they have a different origin. The first is a medium-effect, the second relates to internal degrees of freedom of the particles. Either or both may be relevant for a specific system in nature. In either case there will for example be the same energy vs density functional.

## 6 Appendix B

The scattering phaseshift is related to the reactance matrix in Appendix A. For a rank-1 separable potential one finds

$$< k | \mathcal{R}(\omega = s) | k > = \frac{v^2(k)}{\mathcal{I}(s)}\tag{22}$$

In the Unitary limit  $\mathcal{I}(s)$  is given by eq. (12) with  $s < 0$  in the Faddeev equation, eq. (13). But for free space 2-body scattering one has  $s = k^2$  so that with momenta  $k < 1$  (in units of  $\Lambda$ ) one will have  $0 < s < 1$ . The integral, can again be done analytically and yields

$$\mathcal{I}(0 < s < 1) = 0$$

so that the Reactance matrix element

$$\langle k|\mathcal{R}|k\rangle = \frac{1}{k} \tan \delta(k) \rightarrow \infty$$

i.e.  $\delta(k) = \frac{\pi}{2}$  for ALL momenta  $0 < k < 1$  and the condition for a unitary interaction with a cut-off  $\Lambda$  in momentum-space is satisfied.

## References

- [1] L.D. Faddeev, Zh. Eksperim. Teor. Fiz. **39** (1960) 1459; Sov. Phys. JETP(transl.) **12** (1961) 1014.
- [2] L.H. Thomas, Phys. Rev. **47** (1935) 903.
- [3] V. Efimov, Phys. Lett. **B33** (1970) 903.
- [4] H.D. Amado and J.V. Noble, Phys. Rev. D **5** (1972) 1992.
- [5] P.F. Bedaque, H.-W. Hammer, U. van Kolck, Nucl. Phys. **A646** (1999) 444.
- [6] Eric Braaten, H.-W. Hammer and M.Kusunoki, cond-mat/0206232.
- [7] Eric Braaten, H.-W. Hammer, Physics Reports **428** (2006) 259.
- [8] Eric Braaten, H.-W. Hammer, Ann. of Physics **322** (2007) 120.
- [9] R.F. Mohr, nucl-th/0306086.
- [10] Hans-Werner Hammer and Lucas Platter nucl-th/1102.3789.
- [11] Chen Ji, Daniel R. Phillips and Lucas Platter nucl-th/1106.3837.
- [12] L. Platter and D.R. Phillips Few Body Syst. **40** (2006) 35.
- [13] H.S. Köhler , nucl-th/1012.2926.
- [14] Frank Tabakin, Phys. Rev. **177** (1969) 1443.
- [15] H.S. Köhler , nucl-th/1008.3884.
- [16] G.E. Brown and A.D. Jackson, "The Nucleon-Nucleon Interaction", North-Holland 1976.
- [17] H.S. Köhler , nucl-th/0907.1539.
- [18] S.A. Moszkowski and B.L.Scott, Ann. of Phys. **11** (1960) 65.
- [19] H.S. Köhler and S.A. Moszkowski, nucl-th/0703093.